Positron Emission Tomography (PET) Imaging with [^{11}C]-Labeled Erlotinib: A Micro-PET Study on Mice with Lung Tumor Xenografts

Ashfaque A. Memon,[1] Steen Jakobsen,[2] Frederik Dagnaes-Hansen,[4] Boe S. Sorensen,[1] Susanne Keiding,[2,3] and Ebba Nexo[1]

[1]Department of Clinical Biochemistry, [2]PET Center, [3]Medical Department V, Aarhus University Hospital, Aarhus Sygehus, Norrebrogade, and [4]Department of Medical Microbiology and Immunology, Aarhus University, Aarhus, Denmark

Abstract

Erlotinib (Tarceva) targets the epidermal growth factor receptor (EGFR), which is commonly overexpressed in human cancers, including lung cancer. We show that erlotinib can be labeled with [^{11}C] by reacting the normethyl precursor with [^{11}C]-methyl iodide. By using the 3-(4,5-dimethylthiazol-2-yl)-2,5-diphenyltetrazolium bromide proliferation assay, two lung cancer cell lines (A549 and NCI358) were shown to be less sensitive to erlotinib compared with the lung cancer cell line HCC827. This correlated with higher expression and activity of the EGFR in HCC827 cells as compared with the less sensitive cell lines. Micro–positron emission tomography (PET) and biodistribution of erlotinib was performed with [^{11}C]-erlotinib in nude mice bearing xenografts of A549, NCI358, and HCC827 cells. Dynamic micro-PET showed that HCC827 tumors had the highest [^{11}C]-erlotinib uptake and retained the activity significantly longer as compared with A549 and NCI358 tumors. Biodistribution of [^{11}C]-erlotinib in the xenograft models of lung cancer showed the highest accumulation in the liver. In mice carrying the sensitive cancer cells, the accumulation of [^{11}C]-erlotinib was higher in tumors than in the other organs. In contrast, the drug accumulated to a comparable extent in tumors from the less sensitive cancer cells and the other organs. Uptake of [^{11}C]-erlotinib in the tumors was 1.6%, 0.7%, and 3.7% (percentage of injected dose/g), in A549, NCI358, and HCC827 cells, respectively. We show for the first time that [^{11}C]-erlotinib identifies erlotinib-sensitive tumors. These results pave the road for studies examining the benefit of [^{11}C]-erlotinib PET in patients with lung tumors or other tumors overexpressing EGFR. [Cancer Res 2009;69(3):873–8]

Introduction

Lung cancer is one of the leading causes of all cancer deaths (1), but despite much effort, it is still difficult to predict the response and clinical outcome of the disease. Various treatment strategies, such as surgery, chemotherapy, and radiotherapy have been used for the treatment of patients with lung cancer. In recent years, new treatment strategies targeting the epidermal growth factor receptors (EGFR) have been developed.

The epidermal growth factor (EGF) family of tyrosine kinase receptors consists of four receptors (EGFR, ErbB2, ErbB3, and ErbB4) and more than a dozen ligands (2, 3). Ligand binding to the extracellular domain of the receptor results in the activation of the receptor (4). The activated receptor can dimerize with other EGFRs followed by phosphorylation of tyrosine residues on the receptors (5).

EGFR is one of the most frequently overexpressed proteins in various cancers including lung cancer, and signaling through this receptor has been known to cause tumor progression as well as resistance to different treatments (6–8). Therefore, EGFR has become an attractive target for various treatment strategies. The two most commonly used tyrosine kinase inhibitors targeting EGFR are gefitinib (Iressa, ZD1839) and erlotinib (Tarceva, OSI-774).

Erlotinib and gefitinib are tailored drugs that compete with ATP for the ATP-binding site on the EGFR and thereby prevent phosphorylation and activation of downstream signaling molecules involved in cell proliferation and tumor growth. Gefitinib was the first oral EGFR inhibitor approved for the treatment of advanced non–small cell lung cancer (NSCLC); however, various trials using gefitinib showed that this drug did not significantly prolong survival in the overall study population (9).

In contrast to gefitinib, erlotinib has shown antitumor activity in patients with advanced NSCLC who have failed all prior treatment regimens (10). Erlotinib was also superior to placebo with respect to progression-free survival and objective response rate (11). However, overall response rates have been relatively disappointing (10–15%) in studies that examine all NSCLC patients collectively (12). It is a possibility that not all patients with lung cancer are suitable for erlotinib treatment, and that patients should be selected for this treatment. Various variables have been suggested in order to identify the patients that respond to erlotinib such as type of the tumor, smoking history, gender, and ethnicity (13, 14). Despite this, response rates are not as promising as expected. Expression and mutation status of the EGFR has also been used to predict response, and it has been reported that patients expressing high amounts of the EGFR show better response to erlotinib (12). Furthermore, the presence of specific mutations centered around the ATP binding domain of the receptor has been shown to significantly increase the response to gefitinib treatment in patients with lung cancer (15, 16).

However, analysis of the expression of EGFR and the presence of mutations requires a tumor biopsy, which is not possible to get in all situations. Thus, there is a need to develop noninvasive methods that can identify the subset of patients which are most likely to benefit from erlotinib treatment.

The first prerequisite for a tailored drug to be effective is the binding of the drug with its target. This depends on two major

Requests for reprints: Ashfaque A. Memon, Department of Clinical Biochemistry, AS, Aarhus University Hospital, Norrebrogade 44, 8000 Aarhus C, Denmark. Phone: 45-8949-2911; Fax: 45-8949-3060; E-mail: ashfaque.a.memon@gmail.com.

doi:10.1158/0008-5472.CAN-08-3118

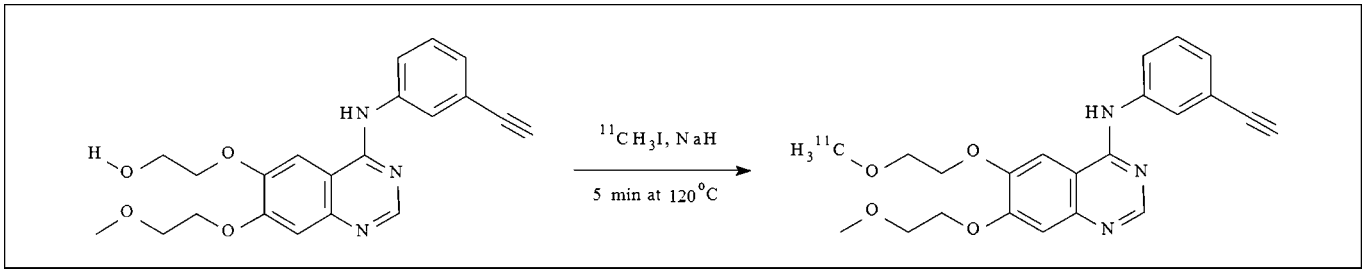

Figure 1. Diagram of [^{11}C]-erlotinib radiosynthesis.

factors (*a*) the presence of the target in the tumor and (*b*) delivery of the drug to the target. Hence, it is important to examine these factors for the selection of patients best-suited for tailored drugs.

Unfortunately, traditional methods of studying kinetics of drug-target interaction are laborious and are not always possible with the clinical material available. Positron emission tomography (PET) has been used to follow the tumor response indirectly by measuring the metabolic activity using [^{18}F]-2-fluoro-2-deoxyglucose in the tumors (17–19). The major challenge with this method is that the high metabolic activity can also be found in other situations such as inflammation, which can produce false-positive results (20). Other strategies such as labeled peptides and antibodies as radiotracers for PET have been used for the diagnosis of the disease or prediction of the response. However, due to the relatively large size and unfavorable receptor binding kinetics compared with systemic clearance of the drug, imaging with these molecules has been hampered (21, 22).

The smaller size and faster systemic clearance of tailored drugs provides a unique opportunity to examine the interaction between the drug and its target EGFR *in vivo*. It has also been shown that labeling of gefitinib with [^{11}C] was possible (23). Therefore, PET imaging with labeled erlotinib may prove to be a useful noninvasive method to screen patients who will respond to erlotinib treatment.

In this study, we have labeled erlotinib with [^{11}C] and have evaluated it as a potential radiotracer for the identification of tumors in mice carrying either sensitive or less sensitive xenografts.

Materials and Methods

Cell lines and reagents. Human lung cancer cell lines, A549, NCI358, and HCC827 were obtained from the American Type Culture Collection. The HCC827 has a high expression of the EGFR and harbors an in-frame deletion mutation (delE746-A750) in exon 19 (24). Cells were grown in DMEM cell culture medium supplemented with 10% fetal bovine serum at 37°C in a humidified atmosphere of 95% air and 5% CO_2 (v/v). Erlotinib hydrochloride and its precursor were provided by OSI Pharmaceuticals.

Western blotting. Western blotting was performed as described before (25). Briefly, lung cancer cells were cultured and harvested at ~80% to 90% confluence, the cell pellet was disrupted on ice for 30 min in radioimmunoprecipitation assay buffer and cleared by centrifugation as described by Schooler and Wiley (26). Protein concentration was determined with a bicinchoninic acid reagent (Pierce Chemical). Equal amounts of protein (25 μg) were resolved by SDS-PAGE. The resolved proteins were transferred onto polyvinylidene difluoride membrane, and blocked with 5% (w/v) nonfat dry milk in TBST solution. The blots were incubated with specific primary and secondary antibodies according to the data sheet provided by the manufacturers. Immunoreactive bands were detected by enhanced chemiluminescence reagents (Amersham Biosciences). Antibody used for Western blotting analysis were p-EGFR (Tyr1173, sc-12351; Santa Cruz Biotechnology), total EGFR (sc-03 Santa Cruz Biotechnology), and actin (Sigma).

Growth inhibition assay. Growth inhibition was assessed by CellTiter 96 nonradioactive cell proliferation assay kit (Promega), a colorimetric method for determining the number of viable cells. Experiments were performed according to the instructions of the manufacturer. Briefly, cells were cultured in 96-well plates and were provided with the kit. The number of cells required for each cell line to obtain an absorbance of 1.3 to 2.2 (linear range of the assay) at a wavelength of 490 nm after 48 h was determined empirically. The number of cells for each cell line was A549

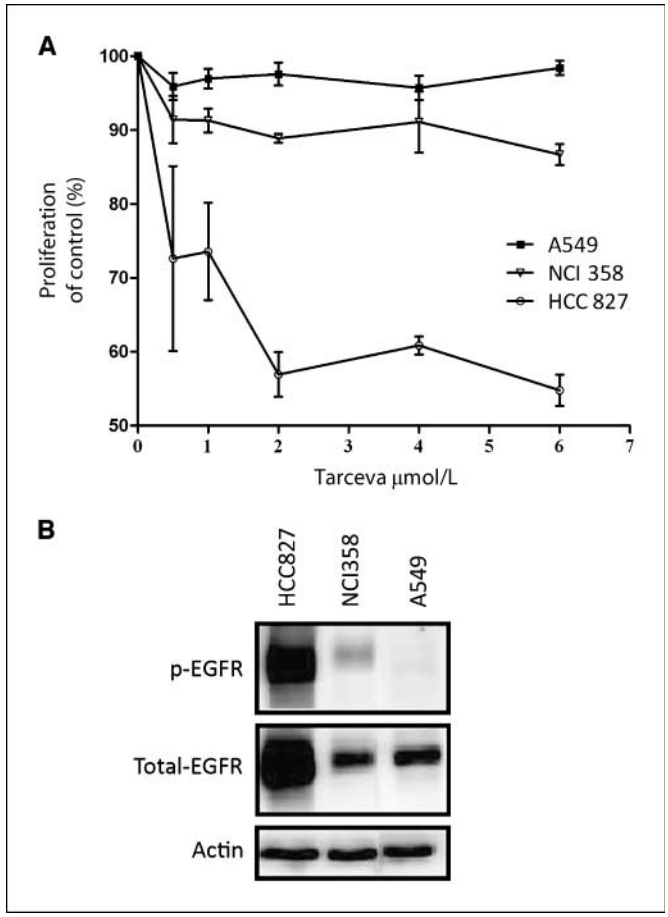

Figure 2. *A,* inhibition of proliferation by erlotinib in lung cancer cells. Cells were treated with erlotinib at the indicated concentrations for 48 h. Viable cells were measured and inhibition of proliferation calculated as the percentage of the control cultures that were only treated with vehicle. *Points,* mean calculated from five replicate wells; *bars,* SD. *B,* expression of phosphorylated and total EGFR in lung cancer cell lines by Western blotting. Actin is shown as a loading control.

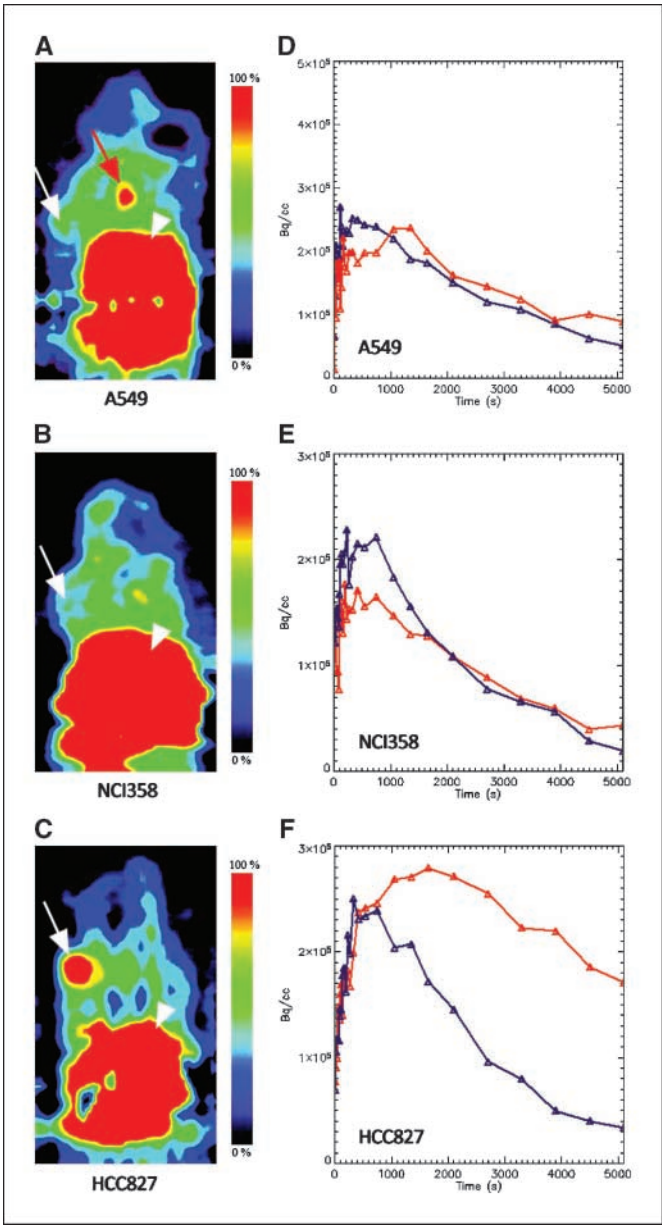

Figure 3. [^{11}C]-erlotinib micro-PET imaging of lung cancer xenografts. Coronal micro-PET images of anesthetized athymic nude mice xenografted with A549 (*A*), NCI358 (*B*), and HCC827 (*C*) lung cancer cells at the left shoulder. Mice were injected with 10 to 15 MBq of [^{11}C]-erlotinib via the lateral tail vein and dynamic scanning was performed for 90 min. *White arrows,* tumors. The hotspot in *A* (*red arrow*) was found in all mice; however, it is not possible to show it in all mice as the tumors are located in different planes. Liver is seen with very high activity with spillover to the surrounding area (*arrowheads*). *Red*, highest signal value; *black*, lowest signal value. *D* to *F,* time-activity curve (TAC), showing activity in tumors compared with the reference area. Regions of interest (ROI) were manually drawn by creating a volume of interest in the central area of the tumor and in the reference area. *Blue lines,* reference area; *red lines,* tumor.

(3,000 cells), and NCI358 and HCC827 (5,000 cells). Twenty-four hours after seeding, cells were treated with 0.5 to 6 μmol/L erlotinib or with vehicle for 48 h.

Labeling of erlotinib. Synthesis of [^{11}C]-erlotinib (Fig. 1) was accomplished by reacting 6-*O*-desmethyl-erlotinib (OSI 420) with [^{11}C]-methyl iodide in dimethyl formamide for 5 min at 120°C, using NaH as the supporting base. The reaction mixture was diluted with high-performance liquid chromatography (HPLC) eluent (46% ethanol, 54% 70 mmol/L sodium dihydrogenphosphate) before injection onto a semi-prep HPLC column (Waters XTerra 5my C18 ODB, 150 × 19 mm) with online UV detection (280 nm) and radiodetection. The fraction corresponding to [*O*-methyl-^{11}C]-erlotinib was collected and transferred to a rotary evaporator, where it was evaporated to near-dryness (100°C under vacuum). The product was reformulated in sterile saline (9 mL) and 100% sterile ethanol (1 mL) and passed through a sterile 0.22 μm filter into a sterile vial. Analytical HPLC (Phenomenex Synergi FUSION 4 μm RP-80, 250 × 4.6 mm, 50% acetonitrile, 50% 70 mmol/L sodium dihydrogen phosphate) showed the product to have <95% radiochemical purity and to have a specific activity in the range of 20 to 100 GBq/μmol.

Lung cancer xenografts and *in vivo* biodistribution studies with [^{11}C]-erlotinib. The animal experiments were approved by the Danish Animal Experiments Inspectorate. Female BALB/cA nude mice (C.Cg/AnBomTac-Foxn^{nu}; Taconic, Ltd.), approximately 8 weeks old, were used for the study. The mice were housed in plastic cages (Tecniplast) under pathogen-free conditions with a 12-h light/12-h dark schedule and fed standard chow (Altromin no. 1324) and water *ad libitum*.

Lung cancer cells were harvested in log phase and were inoculated in the left shoulder subcutaneously. Twenty million cells from each cell line in 200 μL ice-cold PBS were injected per site per animal using a 27-gauge 1/2 mL syringe. By 4 to 5 weeks, tumors were growing exponentially and were ~1 cm in diameter. Xenografts were randomly selected for biodistribution and 15 to 20 MBq of [^{11}C]-erlotinib were injected in each animal model (A549, n = 3; NCI358, n = 3; and HCC827, n = 2) via the lateral tail vein. One hour after injection, animals were sacrificed and the major organs, tumors and blood were weighed and analyzed by a Packard Cobra II γ-counter (Canberra) and the percentage of injected dose per organ per gram (% DPG) were calculated from the tissue count.

Micro-PET imaging with [^{11}C]-erlotinib in lung cancer xenografts. Dynamic micro-PET imaging was performed on lung cancer xenografts for 90 min using a Concorde R4 micro-PET scanner with spatial resolution of 2 mm (Concorde Microsystems). Mice were anesthetized with isoflurane and placed in a polyvinyl chloride tube cut in half longitudinally. Mouse and holder were then positioned in the cavity of the micro-PET scanner. Mice were injected with 10 to 15 MBq of [^{11}C]-erlotinib via the lateral tail vein. Immediately after injection, mice underwent scanning for 90 min while being kept sedated with 1.5% to 2% isoflurane. Body temperature was maintained by a feedback-regulated light bulb connected to a rectal thermo-probe. The frame duration was defined as 8 × 15, 4 × 30, 2 × 60, 2 × 120, 4 × 300 and 6 × 600 s frames. Images were reconstructed from raw data by Fourier rebinning and two-dimensional filtered back projection, resulting in 63 transverse and 128 coronal and sagittal sections with a thickness of 1.2, 0.85, and 0.85 mm, respectively. The images were reconstructed with three-dimensional filtered back projection with a ramp filter with a cutoff frequency of 0.5 pixels^{-1}. No post-filtering or smoothing of the images was performed during or after reconstruction. The PET images were analyzed with the Acquisition Sinogram and Image Processing software that accompanies the Concorde micro-PET. Regions of interest were manually drawn by creating a volume of interest in the central area of the tumor and a reference area. A time-activity curve was plotted for the tumor and the reference area.

Results

Erlotinib sensitivity to lung cancer cell lines related to the expression of EGFR. We analyzed three lung cancer cell lines for their sensitivity to erlotinib. The 3-(4,5-dimethylthiazol-2-yl)-2,5-diphenyltetrazolium bromide proliferation assay showed a significant decrease in the proliferation of HCC827 cells by erlotinib treatment in a dose-dependent manner. In contrast, the A549 and NCI358 cells were less sensitive to erlotinib treatment as concentrations of erlotinib up to 6 μmol/L did not result in a significant decrease in proliferation (Fig. 2*A*). All cell lines were cultured in replicates of five wells and experiments were repeated

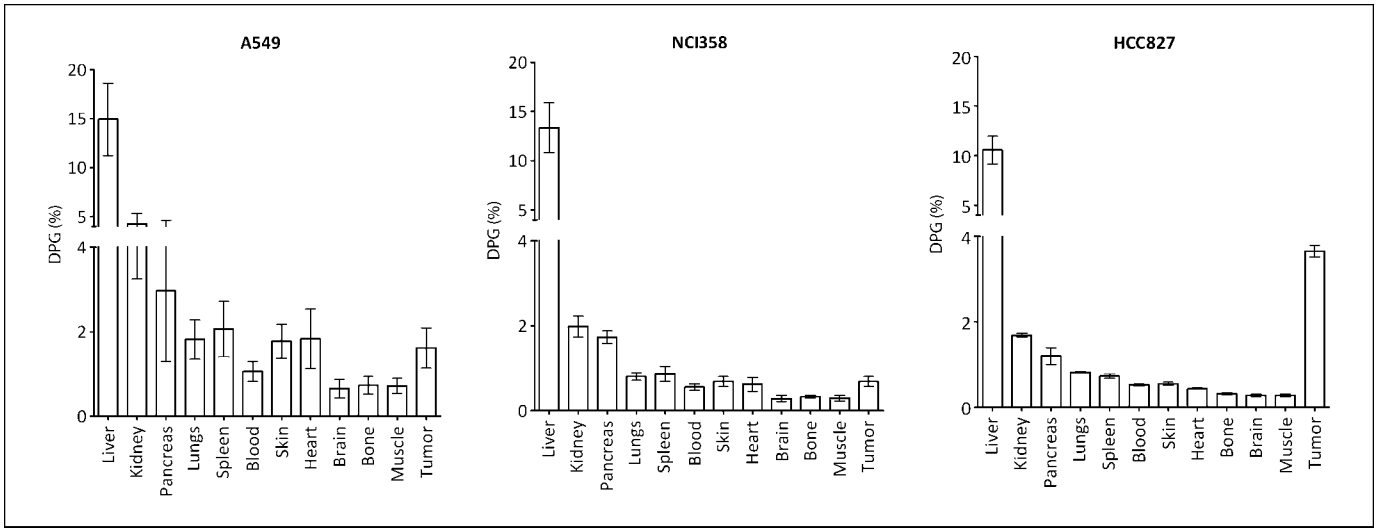

Figure 4. *In vivo* biodistribution of [^{11}C]-erlotinib in lung cancer xenografts. *Columns,* DPG (percentage of injected dose per gram) of [^{11}C]-erlotinib in athymic nude mice bearing subcutaneous A549 (n = 3), NCI358 (n = 3), and HCC827 (n = 2) lung cancer cells.

at least thrice. The data is presented as the percentage of control cells (cells treated with vehicle).

Analysis of EGFR expression by Western blotting showed a high expression of active (phosphorylated) and total EGFR in the sensitive HCC827 cells as compared with the less sensitive A549 and NCI358 cells (Fig. 2*B*).

Micro-PET imaging with [^{11}C]-erlotinib in lung cancer xenografts. Dynamic micro-PET imaging was performed on each tumor model for 90 min after tracer injection (Fig. 3). Tumor is marked by an arrow and a high level of uptake was seen in HCC827 xenografts (Fig. 3*C*), whereas no significant uptake was observed in the A549 and NCI358 xenografts (Fig. 3*A* and *B*, respectively). Furthermore, time-activity curves for tumor and reference area showed that only in the HCC827 xenograft was the activity higher in the tumor than in the reference area throughout the measurement period of 90 min (Fig. 3*F*). The activity was also sustained for a longer time in the HCC827 tumors as compared with the A549 and NCI358 tumors (Fig. 3*D* and *E*, respectively).

***In vivo* biodistribution of [^{11}C]-erlotinib in xenografts.** Biodistribution studies were performed 1 h after injection in xenografts bearing A549 (n = 3), NCI358 (n = 3), and HCC827 (n = 2) lung cancer cells. In all xenograft models, the liver took up the highest amount of activity. In mice xenografts with HCC827 cells, the activity in the tumor was higher than in the other organs measured (apart from the liver), whereas this was not observed when the mice were xenografted with A549 and NCI358 cells (Fig. 4). Tumor accumulation was calculated as 1.62% (±0.47%), 0.69% (±0.11%), and 3.66% (±0.14%) of the injected dose per gram in A549, NCI358, and HCC827 cells, respectively. Table 1 shows the biodistribution of [^{11}C]-erlotinib in all major tissues and all tumors examined in this study. Comparison of the accumulation of [^{11}C]-erlotinib in tumors show a significantly higher activity in HCC827 compared with A549 ($P < 0.05$) or NCI358 ($P < 0.005$), whereas no significant ($P > 0.05$) difference was observed in the accumulation of activity between A549 and NCI358 (Fig. 5).

Discussion

The data presented in this study show for the first time the feasibility of labeling erlotinib and using [^{11}C]-erlotinib as a

Table 1. [^{11}C]-Erlotinib biodistribution (% dose/g) 1 h post–i.v. injection in nude mice bearing lung cancer tumors

Tissue	A549, mean ± SE (n = 3)	NCI358, mean ± SE (n = 3)	HCC827, mean ± SE (n = 2)
Blood	1.06 ± 0.24	0.56 ± 0.08	0.53 ± 0.03
Brain	0.66 ± 0.22	0.29 ± 0.07	0.28 ± 0.02
Muscle	0.72 ± 0.18	0.29 ± 0.07	0.28 ± 0.03
Lungs	1.82 ± 0.46	0.80 ± 0.09	0.82 ± 0.02
Heart	1.84 ± 0.70	0.62 ± 0.16	0.44 ± 0.02
Bone	0.73 ± 0.20	0.33 ± 0.03	0.32 ± 0.03
Pancreas	2.97 ± 1.67	1.73 ± 0.15	1.20 ± 0.20
Spleen	2.06 ± 0.65	0.87 ± 0.18	0.73 ± 0.05
Kidney	4.28 ± 1.03	1.98 ± 0.24	1.69 ± 0.04
Skin	1.78 ± 0.40	0.68 ± 0.12	0.55 ± 0.04
Liver	14.94 ± 3.73	13.34 ± 2.51	10.55 ± 1.47
Tumor	1.62 ± 0.47	0.69 ± 0.11	3.66 ± 0.14

radiotracer. Our results show that [11C]-erlotinib can be used to identify erlotinib-sensitive tumors.

Three human lung cancer cell lines expressing low (A549 and NCI358) and high (HCC827) EGFR were selected for this study. A549 and HCC827 have been characterized as less sensitive and sensitive cell lines, respectively, to treatment with gefitinib (27), which is another EGFR inhibitor with a similar mechanism of action as erlotinib. In agreement with the data on gefitinib sensitivity, a significant decrease in proliferation of HCC827 cells was observed in a dose-dependent manner, whereas A549 was less sensitive to erlotinib treatment and so was the NCI358 cell line.

To evaluate the efficiency of [11C]-erlotinib as a radiotracer, micro-PET scanning on xenografts bearing A549, NCI358, and HCC827 lung cancer cells was performed. This showed that xenografts from the erlotinib-sensitive HCC827 cells could be visualized by micro-PET scanning, whereas xenografts from A549 and NCI358 cells could not. This result was confirmed by biodistribution analysis that showed a higher uptake of [11C]-erlotinib in HCC827 cells as compared with the A549 and NCI358 cells. It is important to note that HCC827 cells have both a high expression of EGFR and also harbor an in-frame deletion mutation (delE746-A750) in exon 19. The presence of this mutation is believed to further increase the sensitivity of the HCC827 cells to erlotinib treatment (24), although the exact mechanism of this increased sensitivity is not fully known. Interestingly, our results obtained from the time-activity curves showed a sustained activity in HCC827 tumors compared with the reference area. It is therefore possible that the presence of this sensitizing mutation might increase the binding of the drug with its target and thereby more efficiently inhibit signaling through EGFR. However, from our data, we cannot conclude whether it is the elevated expression or the mutation that causes the accumulation of erlotinib in the tumor. Nevertheless, our data show that [11C]-erlotinib accumulates in the tumor that responds to erlotinib treatment.

For biodistribution studies, activity was analyzed in the major organs 1 hour after [11C]-erlotinib injection. As expected, the liver showed the highest uptake of the drug as it is the major organ of erlotinib metabolism (28). Interestingly, very little or no activity was measured in the brain. The result is in agreement with previous data indicating that the normal brain expresses low EGFR (29). Therefore, low uptake of [11C]-erlotinib in the brain offers considerable promise for this radiotracer in identifying primary or metastatic brain tumors expressing the EGFR with minimal background. Such tumors have previously been shown to respond to erlotinib (30, 31) and it is therefore very likely that the tumors accumulate the drug.

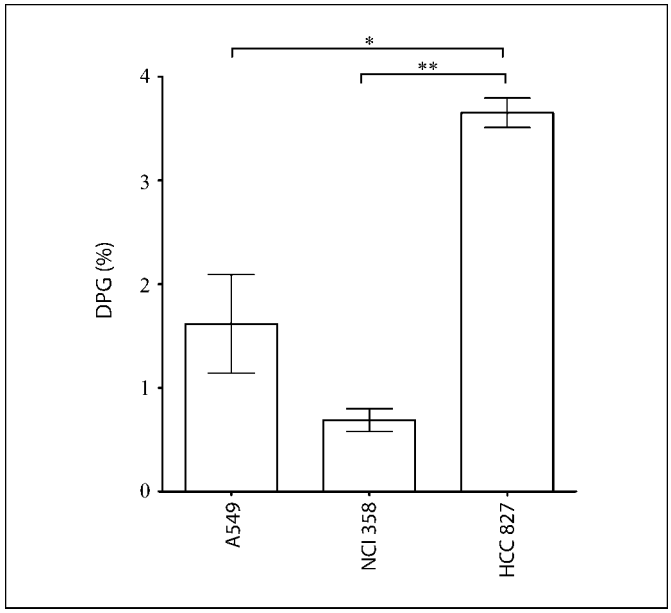

Figure 5. Comparison of [11C]-erlotinib uptake in A549, NCI358, and HCC827 tumors in mice xenografts. *Columns,* DPG (percentage of injected dose per gram) of [11C]-erlotinib in athymic nude mice bearing subcutaneous A549 ($n = 3$), NCI358 ($n = 3$), and HCC827 ($n = 2$) lung cancer cells. *, $P < 0.05$ and **, $P < 0.005$ as determined by t test.

In conclusion, we have developed a method for radiosynthesis of [11C]-erlotinib and evaluated it as a new radiotracer for the identification of tumors sensitive to erlotinib treatment. Our results suggest that [11C]-erlotinib can be used as a noninvasive and rapid method for the identification of erlotinib-responding tumors.

Disclosure of Potential Conflicts of Interest

No potential conflicts of interest were disclosed.

Acknowledgments

Received 8/13/2008; revised 11/3/2008; accepted 11/18/2008.

Grant support: Danish Research Medical Council, NovoNordisk Foundation, the Danish Cancer Society and the Danish Cancer Fund.

The costs of publication of this article were defrayed in part by the payment of page charges. This article must therefore be hereby marked *advertisement* in accordance with 18 U.S.C. Section 1734 solely to indicate this fact.

We thank Alice Villemoes, Birgit Mortensen, Mette Simonsen, and Maciej Bogdan Maniecki of the University Hospital of Aarhus for excellent technical assistance; and OSI pharmaceuticals for providing us the erlotinib and its precursor.

References

1. Parkin DM, Bray F, Ferlay J, Pisani P. Global cancer statistics, 2002. CA Cancer J Clin 2005;55:74–108.
2. Gullick WJ. The type 1 growth factor receptors and their ligands considered as a complex system. Endocr Relat Cancer 2001;8:75–82.
3. Yarden Y, Sliwkowski MX. Untangling the ErbB signalling network. Nat Rev Mol Cell Biol 2001;2:127–37.
4. Burden S, Yarden Y. Neuregulins and their receptors: a versatile signaling module in organogenesis and oncogenesis. Neuron 1997;18:847–55.
5. Hynes NE, Lane HA. ERBB receptors and cancer: the complexity of targeted inhibitors. Nat Rev Cancer 2005;5:341–54.
6. Ciardiello F, Tortora G. EGFR antagonists in cancer treatment. N Engl J Med 2008;358:1160–74.
7. Fontanini G, De Laurentiis M, Vignati S, et al. Evaluation of epidermal growth factor-related growth factors and receptors and of neoangiogenesis in completely resected stage I-IIIA non-small-cell lung cancer: amphiregulin and microvessel count are independent prognostic indicators of survival. Clin Cancer Res 1998;4:241–9.
8. Rusch V, Baselga J, Cordon-Cardo C, et al. Differential expression of the epidermal growth factor receptor and its ligands in primary non-small cell lung cancers and adjacent benign lung. Cancer Res 1993;53:2379–85.
9. Comis RL. The current situation: erlotinib (Tarceva) and gefitinib (Iressa) in non-small cell lung cancer. Oncologist 2005;10:467–70.
10. Shepherd FA, Pereira J, Ciuleanu TE, et al. A randomized placebo-controlled trial of erlotinib in patients with advanced non-small cell lung cancer (NSCLC) following failure of 1(st) line or 2(nd) line chemotherapy. A National Cancer Institute of Canada Clinical Trials Group (NCIC CTG) trial. J Clin Oncol 2004;22:622S.

11. Cohen MH, Johnson JR, Chen YF, Sridhara R, Pazdur R. FDA drug approval summary: erlotinib (Tarceva) tablets. Oncologist 2005;10:461–6.
12. Shepherd FA, Pereira JR, Ciuleanu T, et al. Erlotinib in previously treated non-small-cell lung cancer. N Engl J Med 2005;353:123–32.
13. Fukuoka M, Yano S, Giaccone G, et al. Multi-institutional randomized phase II trial of gefitinib for previously treated patients with advanced non-small-cell lung cancer. J Clin Oncol 2003;21:2237–46.
14. Perez-Soler R, Chachoua A, Hammond LA, et al. Determinants of tumor response and survival with erlotinib in patients with non-small-cell lung cancer. J Clin Oncol 2004;22:3238–47.
15. Lynch TJ, Bell DW, Sordella R, et al. Activating mutations in the epidermal growth factor receptor underlying responsiveness of non-small-cell lung cancer to gefitinib. N Engl J Med 2004;350:2129–39.
16. Paez JG, Janne PA, Lee JC, et al. EGFR mutations in lung cancer: correlation with clinical response to gefitinib therapy. Science 2004;304:1497–500.
17. Gambhir SS. Molecular imaging of cancer with positron emission tomography. Nat Rev Cancer 2002;2:683–93.
18. Jerusalem G, Hustinx R, Beguin Y, Fillet G. PET scan imaging in oncology. Eur J Cancer 2003;39:1525–34.
19. Rohren EM, Turkington TG, Coleman RE. Clinical applications of PET in oncology. Radiology 2004;231:305–32.
20. Love C, Tomas MB, Tronco GG, Palestro CJ. FDG PET of infection and inflammation. Radiographics 2005;25:1357–68.
21. Smith SV. Molecular imaging with copper-64. J Inorg Biochem 2004;98:1874–901.
22. Wu AM, Senter PD. Arming antibodies: prospects and challenges for immunoconjugates. Nat Biotechnol 2005;23:1137–46.
23. Wang JQ, Gao M, Miller KD, Sledge GW, Zheng QH. Synthesis of [^{11}C]Iressa as a new potential PET cancer imaging agent for epidermal growth factor receptor tyrosine kinase. Bioorg Med Chem Lett 2006;16:4102–6.
24. Chang JW, Chou CL, Huang SF, et al. Erlotinib response of EGFR-mutant gefitinib-resistant non-small-cell lung cancer. Lung Cancer 2007;58:414–7.
25. Memon AA, Sorensen BS, Nexo E. The epidermal growth factor family has a dual role in deciding the fate of cancer cells. Scand J Clin Lab Invest 2006;66:623–30.
26. Schooler K, Wiley HS. Ratiometric assay of epidermal growth factor receptor tyrosine kinase activation. Anal Biochem 2000;277:135–42.
27. Mukohara T, Engelman JA, Hanna NH, et al. Differential effects of gefitinib and cetuximab on non-small-cell lung cancers bearing epidermal growth factor receptor mutations. J Natl Cancer Inst 2005;97:1185–94.
28. Ling J, Johnson KA, Miao Z, et al. Metabolism and excretion of erlotinib, a small molecule inhibitor of epidermal growth factor receptor tyrosine kinase, in healthy male volunteers. Drug Metab Dispos 2006;34:420–6.
29. Liu TF, Tatter SB, Willingham MC, Yang M, Hu JJ, Frankel AE. Growth factor receptor expression varies among high-grade gliomas and normal brain: epidermal growth factor receptor has excellent properties for interstitial fusion protein therapy. Mol Cancer Ther 2003;2:783–7.
30. Gounant V, Wislez M, Poulot V, et al. Subsequent brain metastasis responses to epidermal growth factor receptor tyrosine kinase inhibitors in a patient with non-small-cell lung cancer. Lung Cancer 2007;58:425–8.
31. Sarkaria JN, Yang L, Grogan PT, et al. Identification of molecular characteristics correlated with glioblastoma sensitivity to EGFR kinase inhibition through use of an intracranial xenograft test panel. Mol Cancer Ther 2007;6:1167–74.